

# Heavy-to-light semileptonic decays of $\Lambda_b$ and $\Lambda_c$ baryons in the covariant confined quark model

Thomas Gutsche,<sup>1</sup> Mikhail A. Ivanov,<sup>2</sup> Jürgen G. Körner,<sup>3</sup> Valery E. Lyubovitskij,<sup>1,4,5</sup> and Pietro Santorelli<sup>6,7</sup>

<sup>1</sup>Institut für Theoretische Physik, Universität Tübingen, Kepler Center for Astro and Particle Physics,  
Auf der Morgenstelle 14, D-72076 Tübingen, Germany

<sup>2</sup>Bogoliubov Laboratory of Theoretical Physics, Joint Institute for Nuclear Research,  
141980 Dubna, Russia

<sup>3</sup>PRISMA Cluster of Excellence, Institut für Physik, Johannes Gutenberg-Universität,  
D-55099 Mainz, Germany

<sup>4</sup>Department of Physics, Tomsk State University, 634050 Tomsk, Russia

<sup>5</sup>Mathematical Physics Department, Tomsk Polytechnic University,  
Lenin Avenue 30, 634050 Tomsk, Russia

<sup>6</sup>Dipartimento di Scienze Fisiche, Università di Napoli Federico II, Complesso Universitario  
di Monte Sant' Angelo, Via Cintia, Edificio 6, 80126 Napoli, Italy

<sup>7</sup>Istituto Nazionale di Fisica Nucleare, Sezione di Napoli, 80126 Napoli, Italy  
(Received 23 October 2014; published 30 December 2014)

We present a detailed analysis of the heavy-to-light semileptonic decays of the  $\Lambda_b$  and  $\Lambda_c$  baryons  $\Lambda_b \rightarrow p\ell^-\bar{\nu}_\ell$  and  $\Lambda_c \rightarrow n\ell^+\nu_\ell$  in the covariant confined quark model. We calculate the invariant and helicity amplitudes of the two processes which are then used to analyze their angular decay distributions, their rates and asymmetry parameters.

DOI: 10.1103/PhysRevD.90.114033

PACS numbers: 12.39.Ki, 13.30.Eg, 14.20.Jn, 14.20.Mr

## I. INTRODUCTION

Heavy-to-light semileptonic decays of heavy baryons are important physical processes for the determination of the Cabibbo-Kobayashi-Maskawa (CKM) matrix elements. In particular, a study of the exclusive decay  $\Lambda_b \rightarrow p\mu^-\bar{\nu}_e$  at the Large Hadron Collider (LHC) affords the opportunity to determine the CKM matrix element  $|V_{ub}|$ . A discrepancy between the extractions of  $|V_{ub}|$  from the exclusive and inclusive semileptonic  $B$  meson decays at the  $B$  factories [1] is a long-standing puzzle in the heavy flavor sector of the Standard Model. Presently, the Particle Data Group [1] reports the following averaged values for  $|V_{ub}|$ :

$$\begin{aligned} |V_{ub}|_{\text{excl}} &= (4.41 \pm 0.15^{+0.15}_{-0.17}) \times 10^{-3}, \\ |V_{ub}|_{\text{incl}} &= (3.23 \pm 0.3) \times 10^{-3}. \end{aligned} \quad (1)$$

The exclusive result for  $|V_{ub}|$  was extracted from using data from the Belle [2] and *BABAR* [3] Collaborations for the semileptonic  $\bar{B} \rightarrow \pi^+\ell^-\bar{\nu}_\ell$  decay rate together with calculations for the  $B \rightarrow \pi$  transition form factors in lattice QCD [4]. Compared to the  $B$  meson semileptonic decays the baryon transition  $\Lambda_b \rightarrow p$  has an edge over the meson decay because the final state proton has a very distinct experimental signature. It is therefore important to provide a thorough theoretical decay analysis of the decay  $\Lambda_b \rightarrow p\ell^-\bar{\nu}_\ell$  starting from a determination of the vector and axial form factors describing the current-induced  $\Lambda_b \rightarrow p$  transition matrix element. The calculation of the  $\Lambda_b \rightarrow p$  form factors has been performed before using different versions

of QCD sum rules [5–10], quark models [11–14] and lattice QCD [15]. In this paper we present calculations for the form factors characterizing the  $\Lambda_b \rightarrow p\ell^-\bar{\nu}_\ell$  and  $\Lambda_c \rightarrow n\ell^+\nu_\ell$  transitions covariant confined quark model [16–23].

## II. $\Lambda_b \rightarrow p\ell^-\bar{\nu}_\ell$ AND $\Lambda_c \rightarrow n\ell^+\nu_\ell$ MATRIX ELEMENTS AND OBSERVABLES

The effective Fermi Lagrangian for the semileptonic transitions  $b \rightarrow u\ell^-\bar{\nu}_\ell$  and  $c \rightarrow d\ell^+\nu_\ell$  reads

$$\begin{aligned} \mathcal{L}_{\text{eff}} = \frac{G_F}{\sqrt{2}} &\left[ V_{ub}(\bar{u}^a O_\mu b^a)(\bar{\ell}^a O^\mu \nu_\ell) \right. \\ &\left. + V_{cd}(\bar{c}^a O_\mu d^a)(\bar{\ell}^a O^\mu \nu_\ell) \right] + \text{H.c.}, \end{aligned} \quad (2)$$

where  $O_\mu = \gamma_\mu(1 - \gamma_5)$  and  $V_{qq'}$  are the Kobayashi-Maskawa matrix elements ( $|V_{ub}| = 0.00389$ ,  $|V_{cd}| = 0.230$ ).

This Lagrangian generates transitions on the quark level which in turn determine the heavy-to-light baryon transition matrix elements. The corresponding matrix elements of the exclusive transition  $\Lambda_b \rightarrow p\ell^-\bar{\nu}_\ell$  and  $\Lambda_c \rightarrow n\ell^+\nu_\ell$  are defined by

$$\begin{aligned} M(\Lambda_b \rightarrow p\ell^-\bar{\nu}_\ell) &= \frac{G_F}{\sqrt{2}} V_{ub} \langle p | \bar{u} O_\mu b | \Lambda_b \rangle j_\ell^\mu, \\ M(\Lambda_c \rightarrow n\ell^+\nu_\ell) &= \frac{G_F}{\sqrt{2}} V_{cd}^* \langle n | \bar{d} O_\mu c | \Lambda_c \rangle j_\ell^\mu, \end{aligned} \quad (3)$$

where  $j_\ell^\mu$  is the leptonic current formed by the corresponding charged lepton and (anti)neutrino.

The hadronic matrix elements  $\langle p|\bar{u}O_\mu b|\Lambda_b\rangle$  and  $\langle n|\bar{d}O_\mu c|\Lambda_c\rangle$  in (3) can be written in terms of six dimensionless, invariant form factors  $f_i^J$  ( $i = 1, 2, 3$  and  $J = V, A$ ), viz.

$$\begin{aligned}\langle B_2|\bar{s}\gamma^\mu b|B_1\rangle &= \bar{u}_2(p_2)[f_1^V(q^2)\gamma^\mu - f_2^V(q^2)i\sigma^{\mu q}/M_1 \\ &\quad + f_3^V(q^2)q^\mu/M_1]u_1(p_1), \\ \langle B_2|\bar{s}\gamma^\mu\gamma^5 b|B_1\rangle &= \bar{u}_2(p_2)[f_1^A(q^2)\gamma^\mu - f_2^A(q^2)i\sigma^{\mu q}/M_1 \\ &\quad + f_3^A(q^2)q^\mu/M_1]\gamma^5 u_1(p_1),\end{aligned}\quad (4)$$

where  $q = p_1 - p_2$ . Since we will also discuss lepton mass effects, it is necessary to include the scalar form factors  $f_3^V$  and  $f_3^A$  in the expansion (4). The details of how to calculate the six form factors in the covariant confined quark model approach was discussed in our previous paper [22,23].

It is convenient to analyze the semileptonic decays of heavy baryons in terms of helicity amplitudes  $H_{\lambda_2\lambda_j}$  which are linearly related to the invariant form factors  $f_i^V$  and  $f_i^A$  (see details in Refs. [22–26]). Here we shall employ a generic notation such that the parent and daughter baryons are denoted by  $B_1$  and  $B_2$ . The helicities of the daughter

baryon  $B_2$  and the effective current are denoted by  $\lambda_2$  and  $\lambda_j$ , respectively. The pertinent relation is

$$H_{\lambda_2\lambda_j} = \langle B_2(\lambda_2)|\bar{q}'O_\mu q|B_1(\lambda_1)\rangle e^{\dagger\mu}(\lambda_j) = H_{\lambda_2\lambda_j}^V - H_{\lambda_2\lambda_j}^A. \quad (5)$$

The helicity amplitudes have been split into their vector ( $H_{\lambda_2\lambda_j}^V$ ) and axial-vector ( $H_{\lambda_2\lambda_j}^A$ ) parts. We shall work in the rest frame of the parent baryon  $B_1$  with the daughter baryon  $B_2$  moving in the negative  $z$  direction such that  $p_1^\mu = (M_1, \mathbf{0})$ ,  $p_2^\mu = (E_2, 0, 0, -|\mathbf{p}_2|)$  and  $q^\mu = (q_0, 0, 0, |\mathbf{p}_2|)$ . Further we use the following definitions of kinematical variables  $q_0 = (M_+M_- + q^2)/(2M_1)$ ,  $|\mathbf{p}_2| = \sqrt{Q_+Q_-}/2M_1$  and  $E_2 = M_1 - q_0 = (M_1^2 + M_2^2 - q^2)/(2M_1)$ , where  $q^2$  is the momentum squared transferred to the leptonic pair. We have introduced the notation  $M_\pm = M_1 \pm M_2$ ,  $Q_\pm = M_\pm^2 - q^2$ . Angular momentum conservation fixes the helicity  $\lambda_1$  of the parent baryon such that  $\lambda_1 = -\lambda_2 + \lambda_j$ . The relations between the helicity amplitudes  $H_{\lambda_2\lambda_j}^{V,A}$  and the invariant amplitudes are given by [22,23]

$$\begin{aligned}H_{\pm\frac{1}{2}\pm 1}^V &= \sqrt{2Q_-}\left(f_1^V + \frac{M_+}{M_1}f_2^V\right), & H_{\pm\frac{1}{2}\pm 1}^A &= \pm\sqrt{2Q_+}\left(f_1^A - \frac{M_-}{M_1}f_2^A\right), \\ H_{\pm\frac{1}{2}0}^V &= \sqrt{\frac{Q_-}{q^2}}\left(M_+f_1^V + \frac{q^2}{M_1}f_2^V\right), & H_{\pm\frac{1}{2}0}^A &= \pm\sqrt{\frac{Q_+}{q^2}}\left(M_-f_1^A - \frac{q^2}{M_1}f_2^A\right), \\ H_{\pm\frac{1}{2}\pm t}^V &= \pm\sqrt{\frac{Q_+}{q^2}}\left(M_-f_1^V + \frac{q^2}{M_1}f_3^V\right), & H_{\pm\frac{1}{2}\pm t}^A &= \pm\sqrt{\frac{Q_-}{q^2}}\left(M_+f_1^A - \frac{q^2}{M_1}f_3^A\right).\end{aligned}\quad (6)$$

The scalar helicity component is denoted by  $\lambda_j = t$ . The scalar helicity amplitudes contribute only for nonzero charged lepton masses. As in Ref. [22] we introduce the following combinations of helicity amplitudes:

$$\begin{aligned}H_U &= |H_{\frac{1}{2}1}|^2 + |H_{-\frac{1}{2}-1}|^2 && \text{transverse unpolarized (pc),} \\ H_L &= |H_{\frac{1}{2}0}|^2 + |H_{-\frac{1}{2}0}|^2 && \text{longitudinal unpolarized (pc),} \\ H_S &= |H_{\frac{1}{2}t}|^2 + |H_{-\frac{1}{2}t}|^2 && \text{scalar unpolarized (pc).} \\ H_P &= |H_{\frac{1}{2}1}|^2 - |H_{-\frac{1}{2}-1}|^2 && \text{transverse parity-odd polarized (pv),} \\ H_{L_p} &= |H_{\frac{1}{2}0}|^2 - |H_{-\frac{1}{2}0}|^2 && \text{longitudinal polarized (pv),} \\ H_{S_p} &= |H_{\frac{1}{2}t}|^2 - |H_{-\frac{1}{2}t}|^2 && \text{scalar polarized (pv),} \\ H_{LS} &= H_{\frac{1}{2}1}H_{\frac{1}{2}0} + H_{-\frac{1}{2}-1}H_{-\frac{1}{2}0} && \text{longitudinal-scalar interference (pc).}\end{aligned}\quad (7)$$

We have indicated the parity properties of the seven combinations in round brackets. The partial helicity width  $\Gamma_I$  and branching ratio  $B_I$  corresponding to one of the seven specific combinations of differential helicity amplitudes in (7) are defined as

$$\Gamma_I = \int_{m_\ell^2}^{M^2} dq^2 \frac{d\Gamma_I}{dq^2}, \quad B_I = \Gamma_I \tau, \quad \frac{d\Gamma_I}{dq^2} = \frac{1}{2}(2\pi)^3 |V_{Qq}|^2 \frac{|\mathbf{p}_2|}{12M_1^2} q^2 \left(1 - \frac{m_\ell^2}{q^2}\right)^2 H_I, \quad I = U, L, S, P, L_p, S_p, LS, \quad (8)$$

where  $\tau$  is the lifetime of the parent baryon:  $\tau_{\Lambda_b} = 1.425 \times 10^{-12}$  s and  $\tau_{\Lambda_c} = 0.2 \times 10^{-12}$  s. For the  $\Lambda_b \rightarrow p + \ell^- \bar{\nu}_\ell$  and  $\Lambda_c \rightarrow n + \ell^+ \nu_\ell$  decay widths and the asymmetry parameter  $\alpha_{FB}^\ell$  [forward-backward asymmetry of the charged leptons in the  $W^-$  off-shell rest frame or in the  $(\ell, \nu_\ell)$  c.m. frame] one finds [26]

$$\Gamma = \int_{m_\ell^2}^{M^2} dq^2 \frac{d\Gamma}{dq^2},$$

$$d\Gamma = d\Gamma_U + d\Gamma_L + \frac{m_\ell^2}{2q^2} (d\Gamma_U + d\Gamma_L + 3d\Gamma_S) \quad (9)$$

and

$$\alpha_{FB}^\ell = \frac{\tilde{\Gamma}}{\Gamma}, \quad \tilde{\Gamma} = \int_{m_\ell^2}^{M^2} dq^2 \frac{d\tilde{\Gamma}}{dq^2},$$

$$d\tilde{\Gamma} = \frac{3}{4} \left\{ \pm d\Gamma_P - \frac{2m_\ell^2}{q^2} d\Gamma_{LS} \right\}. \quad (10)$$

where the plus/minus signs refer to the  $\Lambda_b \rightarrow p \ell^- \bar{\nu}_\ell$  and  $\Lambda_c \rightarrow n \ell^+ \nu_\ell$  cases, respectively [26].

### III. THE $\Lambda_Q \rightarrow N$ TRANSITIONS IN THE COVARIANT CONFINED QUARK MODEL

For the description of the couplings of the heavy baryons  $\Lambda_Q$  ( $Q = b, c$ ) and nucleons to their constituent quarks we employ generic Lagrangians which [12,20,27]

---


$$\Lambda_Q: \mathcal{L}_{int}^{\Lambda_Q}(x) = g_{\Lambda_Q} \bar{\Lambda}_Q(x) \cdot J_{\Lambda_Q}(x) + \text{H.c.},$$

$$J_{\Lambda_Q}(x) = \int dx_1 \int dx_2 \int dx_3 F_{\Lambda_Q}(x; x_1, x_2, x_3) \epsilon^{a_1 a_2 a_3} Q^{a_1}(x_1) u^{a_2}(x_2) C \gamma^5 d^{a_3}(x_3), \quad (11)$$

$$N: \mathcal{L}_{int}^N(x) = g_N \bar{N}(x) \cdot J_N(x) + \text{H.c.},$$

$$J_N(x) = (1 - x_N) J_N^V + x_N J_N^T,$$

$$J_N^V(x) = \int dx_1 \int dx_2 \int dx_3 F_N(x; x_1, x_2, x_3) \epsilon^{a_1 a_2 a_3} \gamma^\mu \gamma^5 d^{a_1}(x_1) u^{a_2}(x_2) C \gamma_\mu u^{a_3}(x_3),$$

$$J_N^T(x) = \int dx_1 \int dx_2 \int dx_3 F_N(x; x_1, x_2, x_3) \epsilon^{a_1 a_2 a_3} \frac{1}{2} \sigma^{\mu\nu} \gamma^5 d^{a_1}(x_1) u^{a_2}(x_2) C \sigma_{\mu\nu} u^{a_3}(x_3),$$

$$J_n^V(x) = - \int dx_1 \int dx_2 \int dx_3 F_N(x; x_1, x_2, x_3) \epsilon^{a_1 a_2 a_3} \gamma^\mu \gamma^5 u^{a_1}(x_1) d^{a_2}(x_2) C \gamma_\mu d^{a_3}(x_3),$$

$$J_n^T(x) = - \int dx_1 \int dx_2 \int dx_3 F_N(x; x_1, x_2, x_3) \epsilon^{a_1 a_2 a_3} \frac{1}{2} \sigma^{\mu\nu} \gamma^5 u^{a_1}(x_1) d^{a_2}(x_2) C \sigma_{\mu\nu} d^{a_3}(x_3). \quad (12)$$

The color index is denoted by  $a$  and  $C = \gamma^0 \gamma^2$  is the charge conjugation matrix. In the  $\Lambda_Q$  baryon case we take the  $u$  and  $d$  quarks to be in a  $S = 0$  and  $I = 0$  [ $ud$ ] diquark configuration antisymmetric in spin and isospin. In the case of the nucleon we use an interpolating current of the so-called *vector* current variety [20], which contains two  $u$  quarks (in case of the proton) or two  $d$  quarks (in case of the neutron) in a symmetric diquark configuration with spin and isospin equal to 1. Note that these currents are fully symmetric in configuration, spin and isospin space. In particular, using Fierz transformations for spin matrices one can show (see details in Ref. [28] and our explanation below) that these currents can be rewritten in terms of diquark with spin and isospin equal to 0 and in manifestly spin-isospin symmetric form, where nucleon current with both diquark configurations enter with equal weight.

In particular, when constructing interpolating baryon currents it is convenient to use Fierz transformations and

corresponding identities in order to interchange the quark fields. First we specify five possible spin structures

$$J^{\alpha\beta,\rho\sigma} = \Gamma_1^{\alpha\beta} \otimes (C \Gamma_2)^{\rho\sigma} \quad (13)$$

defining the Fierz transformation of the baryon currents,

$$P = I \otimes C \gamma_5,$$

$$S = \gamma_5 \otimes C,$$

$$A = \gamma^\mu \otimes C \gamma_5 \gamma_\mu,$$

$$V = \gamma^\mu \gamma^5 \otimes C \gamma_\mu,$$

$$T = \frac{1}{2} \sigma^{\mu\nu} \gamma^5 \otimes C \sigma_{\mu\nu}. \quad (14)$$

The Fierz transformation of the structures  $J = \{P, S, A, V, T\}$  read

$$\begin{aligned}
P &= \frac{1}{4}(\tilde{P} + \tilde{S} + \tilde{A} + \tilde{V} + \tilde{T}), \\
S &= \frac{1}{4}(\tilde{P} + \tilde{S} - \tilde{A} - \tilde{V} + \tilde{T}), \\
A &= \tilde{P} - \tilde{S} - \frac{1}{2}(\tilde{A} - \tilde{V}), \\
V &= \tilde{P} - \tilde{S} + \frac{1}{2}(\tilde{A} - \tilde{V}), \\
T &= \frac{3}{2}(\tilde{P} + \tilde{S}) - \frac{1}{2}\tilde{T}.
\end{aligned} \tag{15}$$

Next we show that vector and tensor nucleon currents containing diquark with spin and isospin equal to one can be transformed to the currents containing diquark with spin and isospin equal to zero using the symmetry property of the nucleon currents in the configuration space [i.e. the correlation function  $F_N(x; x_1, x_2, x_3)$  is symmetric under permutation of quark coordinates  $x_1, x_2, x_3$ ]. See e.g. how it works for the proton (for the neutron one can proceed by analogy changing  $u \leftrightarrow d$ ),

---


$$\begin{aligned}
J_p^V(x) &= \int dx_1 \int dx_2 \int dx_3 F_N(x; x_1, x_2, x_3) \epsilon^{a_1 a_2 a_3} \gamma^\mu \gamma^5 d^{a_1}(x_1) u^{a_2}(x_2) C \gamma_\mu u^{a_3}(x_3) \\
&= \frac{2}{3} [2J_p^P(x) - 2J_p^S(x) + J_p^A(x)] \\
&= \frac{2}{3} \int dx_1 \int dx_2 \int dx_3 F_N(x; x_1, x_2, x_3) \epsilon^{a_1 a_2 a_3} [2u^{a_1}(x_1) u^{a_2}(x_2) C \gamma_5 d^{a_3}(x_3) - 2\gamma_5 u^{a_1}(x_1) u^{a_2}(x_2) C d^{a_3}(x_3) \\
&\quad + \gamma^\mu u^{a_1}(x_1) u^{a_2}(x_2) C \gamma_\mu \gamma_5 d^{a_3}(x_3)]
\end{aligned} \tag{16}$$

and

$$\begin{aligned}
J_p^T(x) &= \int dx_1 \int dx_2 \int dx_3 F_N(x; x_1, x_2, x_3) \epsilon^{a_1 a_2 a_3} \frac{1}{2} \sigma^{\mu\nu} \gamma^5 d^{a_1}(x_1) u^{a_2}(x_2) C \sigma_{\mu\nu} u^{a_3}(x_3) \\
&= 2[J_p^P(x) + J_p^S(x)] \\
&= 2 \int dx_1 \int dx_2 \int dx_3 F_N(x; x_1, x_2, x_3) \epsilon^{a_1 a_2 a_3} [u^{a_1}(x_1) u^{a_2}(x_2) C \gamma_5 d^{a_3}(x_3) + \gamma_5 u^{a_1}(x_1) u^{a_2}(x_2) C d^{a_3}(x_3)].
\end{aligned} \tag{17}$$

It is clear that nucleon currents can be written in manifestly spin-isospin invariant form containing currents with two possible types of diquarks with equal weight,

$$\begin{aligned}
J_p^{(1)}(x) &= \frac{1}{2} \left[ J_p^V(x) + \frac{2}{3} (2J_p^P(x) - 2J_p^S(x) + J_p^A(x)) \right], \\
J_p^{(2)}(x) &= \frac{1}{2} [J_p^T(x) + 2(J_p^P(x) + J_p^S(x))].
\end{aligned} \tag{18}$$

The nonlocal vertex functions in momentum space are denoted by  $\bar{\Phi}_H(-P^2)$  and are obtained from the Fourier transformations of the vertex functions  $F_H$  entering in Eqs. (11) and (12). In the numerical calculations we choose a simple Gaussian form for the vertex functions (for both mesons and baryons),

$$\bar{\Phi}_H(-P^2) = \exp(P^2/\Lambda_H^2), \tag{19}$$

where  $\Lambda_H$  is a size parameter describing the size of the distribution of the quarks inside a given hadron  $H$ . The values for these parameters were fixed before in [19–23]. We would like to stress that the Minkowskian momentum

variable  $P^2$  turns into the Euclidean form  $-P_E^2$  needed for the appropriate falloff behavior of the correlation function (19) in the Euclidean region. We emphasize that any choice for the correlation function  $\bar{\Phi}_H$  is acceptable as long as it falls off sufficiently fast in the ultraviolet region of Euclidean space. The choice of a Gaussian form for  $\bar{\Phi}_H$  has obvious calculational advantages.

For given values of the size parameters  $\Lambda_H$  the coupling constants  $g_{\Lambda_Q}$  and  $g_N$  are determined by the compositeness condition suggested by Weinberg [29] and Salam [30] (for a review, see [31]) and extensively used in our approach (for details, see [32]). The compositeness condition implies that the renormalization constant of the hadron wave function is set equal to zero,

$$Z_H = 1 - \Sigma'_H = 0, \tag{20}$$

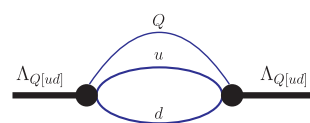


FIG. 1 (color online). Mass operator of  $\Lambda_Q$  baryon.

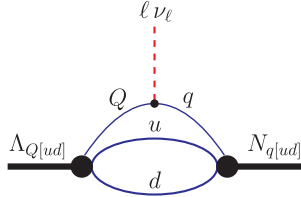


FIG. 2 (color online). Diagrams contributing to the semileptonic decays of  $\Lambda_Q$  baryons.

where  $\Sigma'_H$  is the on-shell derivative of the hadron mass function  $\Sigma_H$  with respect to its momentum. In Fig. 1 we present as an example the diagram corresponding to the mass operator of the  $\Lambda_Q$  baryon. The compositeness condition can be seen to provide for the correct charge normalization for a charged bound state (see e.g. [19]).

How to calculate the matrix element of the baryonic transitions has been discussed in detail in our previous papers [20,22,23]. In our approach semileptonic transitions between baryons are described by a two-loop Feynman-type diagram involving nonlocal vertex functions as shown in Fig. 2.

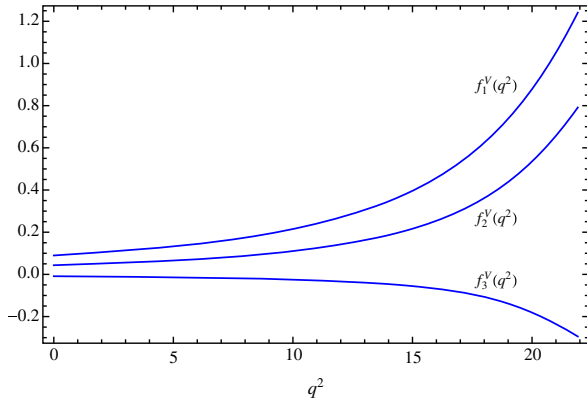


FIG. 3 (color online).  $q^2$  dependence of the vector form factors for the  $\Lambda_b \rightarrow p$  transition.

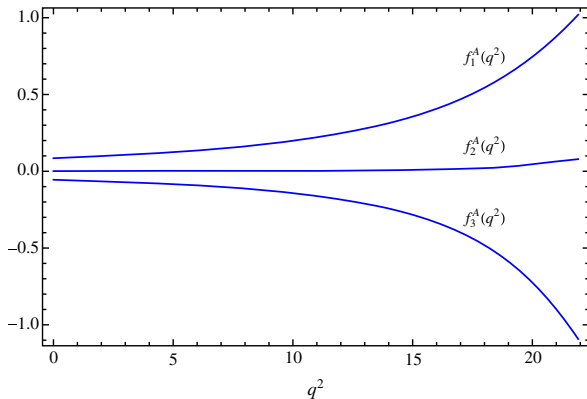


FIG. 4 (color online).  $q^2$  dependence of the axial form factors for the  $\Lambda_b \rightarrow p$  transition.

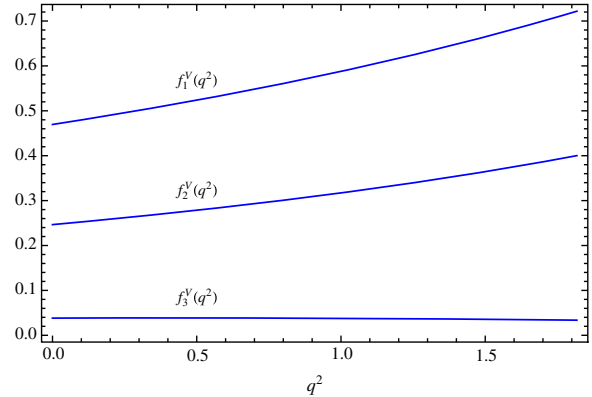


FIG. 5 (color online).  $q^2$  dependence of the vector form factors for the  $\Lambda_c \rightarrow n$  transition.

In the calculation of the quark-loop diagram (Fig. 2) we use the set of model parameters fixed in our previous studies. The model parameters are the constituent quark masses  $m_q$  and the infrared cutoff parameter  $\lambda$  responsible for quark confinement. They are taken from a fit done in the papers [19–21]:

$$\begin{array}{cccccc} m_u & m_s & m_c & m_b & \lambda & \\ 0.235 & 0.424 & 2.16 & 5.09 & 0.181 & \text{GeV} \end{array} \quad (21)$$

It is a big advantage of our approach that we are able to reproduce data on meson and baryon properties with the same (universal) masses of the constituent quarks. The crucial point in such a unified description is taken into account for the quark confinement. Again for all diagrams (matrix elements) in both meson and baryon sectors we use the universal confinement scale.

The dimensional size parameters  $\Lambda$  in Eq. (19) and the dimensionless parameter  $x_N$  in Eq. (12) characterizing the vector and tensor current mixing have been determined in [20,22] by a fit to the magnetic moments of nucleons and to the semileptonic decays  $\Lambda_b \rightarrow \Lambda_c \ell^- \bar{\nu}_\ell$  and  $\Lambda_c \rightarrow \Lambda \ell^+ \nu_\ell$ . The resulting values are

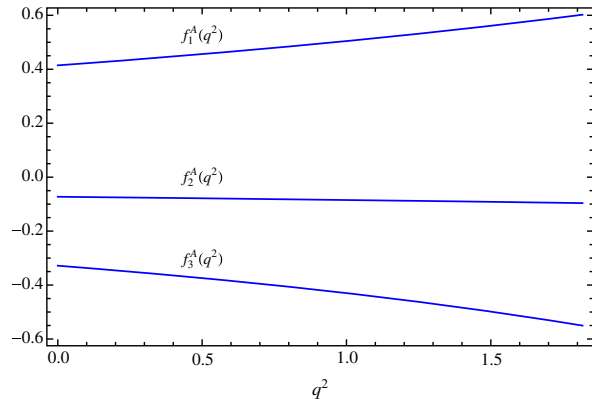


FIG. 6 (color online).  $q^2$  dependence of the axial form factors for the  $\Lambda_c \rightarrow n$  transition.

TABLE I. Parameters for the approximated form factors in Eq. (23) for the  $\Lambda_b \rightarrow p$  transitions.

	$f_1^V$	$f_2^V$	$f_3^V$	$f_1^A$	$f_2^A$	$f_3^A$
$f(0)$	0.090	0.043	-0.009	0.085	0.001	-0.055
$a$	2.262	2.380	2.592	2.213	2.793	2.403
$b$	1.333	1.466	1.720	1.286	1.976	1.491

TABLE II. Parameters for the approximated form factors in Eq. (23) for the  $\Lambda_c \rightarrow n$  transitions.

	$f_1^V$	$f_2^V$	$f_3^V$	$f_1^A$	$f_2^A$	$f_3^A$
$f(0)$	0.470	0.247	0.038	0.414	-0.073	-0.328
$a$	1.111	1.240	0.308	0.978	0.781	1.330
$b$	0.303	0.390	1.998	0.235	0.225	0.486

TABLE III.  $\Lambda_b \rightarrow p$  transitions: Comparison of our form factors at  $q^2 = 0$  and  $q^2 = q_{\max}^2$  with those obtained in [10,14].

		$f_1^V$	$f_2^V$	$f_3^V$	$f_1^A$	$f_2^A$	$f_3^A$
$q^2 = 0$	[10]	$0.12^{+0.03}_{-0.04}$	$0.047^{+0.015}_{-0.013}$	...	$0.12^{+0.03}_{-0.03}$	$-0.016^{+0.007}_{-0.005}$	...
	[14]	0.1131	0.0356	...	0.1112	0.0097	...
$q^2 = q_{\max}^2$	Our	0.080	0.036	-0.005	0.077	-0.001	-0.046
	[14]	0.626	0.231	...	0.581	-0.089	...
	Our	1.254	0.801	-0.300	1.030	0.082	-1.105

TABLE IV.  $\Lambda_c \rightarrow n$  transitions: Comparison of our form factors values at  $q^2 = 0$  and  $q^2 = q_{\max}^2$  to those obtained in [10,14].

		$f_1^V$	$f_2^V$	$f_3^V$	$f_1^A$	$f_2^A$	$f_3^A$
$q^2 = 0$	[10]	$0.59^{+0.15}_{-0.11}$	$0.43^{+0.13}_{-0.12}$	...	$0.55^{+0.14}_{-0.15}$	$-0.16^{+0.08}_{-0.05}$	...
	[14]	0.1081	0.0311	...	0.1065	-0.0064	...
$q^2 = q_{\max}^2$	Our	0.470	0.246	0.039	0.414	-0.073	-0.328
	[14]	0.187	0.0652	...	0.187	-0.0214	...
	Our	0.721	0.400	0.033	0.602	-0.096	-0.550

$$\begin{array}{cccccc} x_N & \Lambda_N & \Lambda_{\Lambda_s} & \Lambda_{\Lambda_c} & \Lambda_{\Lambda_b} & \text{GeV} \end{array} \quad (22)$$

0.8    0.50    0.492    0.867    0.571    GeV

It should be clear that the evaluation of the form factors is technically quite intricate. It involves the calculation of a two-loop Feynman diagram with a complex spin structure resulting from the quark propagators and the vertex functions which leads to a number of two-loop tensor integrals. In order to tackle this difficult task we have automated the calculation in the form of FORM and FORTRAN packages written for this purpose.

The  $q^2$  behavior of the form factors are shown in Figs. (3–6). The results of our numerical calculations are well represented by a double-pole parametrization of the form

$$f(\hat{s}) = f(0) \frac{1}{1 - a\hat{s} + b\hat{s}^2}, \quad (23)$$

where  $\hat{s} = q^2/M_1^2$ . Using such a parametrization accelerates the necessary  $q^2$  integrations which can be done using the

parametrization (23) without having to do a numerical evaluation of the loop diagram for each  $q^2$  value separately. The values of  $f(0)$ ,  $a$  and  $b$  are listed in Tables I and II. Note that the dominant form factors  $f_1^{V/A}$  in Tables I and II are very close to a dipole form since one has  $\sqrt{b} \sim a/2$  in all four cases. The effective dipole mass is given by  $m_{\text{eff}} = M_1/\sqrt{a/2}$  or  $m_{\text{eff}} = M_1/b^{1/4}$ . In the  $\Lambda_b \rightarrow p$  case the effective dipole mass is very close to the average of the  $B$ ,  $B^*$  meson masses. In the

TABLE V. Total  $B(\Lambda_Q \rightarrow N\ell\nu_\ell)$  and partial  $B_I(\Lambda_Q \rightarrow N\ell\nu_\ell)$  helicity contributions to branching ratios (in units of  $10^{-4}$ ).

Mode	Our results			
	$B$	$B_U$	$B_L$	$B_S$
$\Lambda_b \rightarrow p e^- \bar{\nu}_e$	2.9	1.6	1.3	$\simeq 0$
$\Lambda_b \rightarrow p \mu^- \bar{\nu}_\mu$	2.9	1.6	1.3	$\simeq 0$
$\Lambda_b \rightarrow p \tau^- \bar{\nu}_\tau$	2.1	1.0	0.7	0.2
$\Lambda_c \rightarrow n e^+ \nu_e$	20.7	8.3	12.3	$\simeq 0$
$\Lambda_c \rightarrow n \mu^+ \nu_\mu$	20.2	8.1	11.3	0.5

TABLE VI. Decay widths  $\Lambda_b \rightarrow p\ell^-\bar{\nu}_\ell$  (in units of  $|V_{ub}|^2 \text{ ps}^{-1}$ ).

Mode	Our result	Theoretical predictions
$\Lambda_b \rightarrow pe^-\bar{\nu}_e$	13.3	6.48 [11]; 7.47 [12]; 4.55 [13]; 7.55 [13]; 11.8 [14]; $19.0^{+8.6}_{-6.9}$ [10]; $250 \pm 85$ [9]; $235 \pm 85$ [9]; $477 \pm 175$ [9]; $3.76 \pm 1.20$ [9]
$\Lambda_b \rightarrow p\mu^-\bar{\nu}_\mu$	13.3	6.48 [11]; 7.47 [12]; 4.55 [13]; 7.55 [13]; 11.8 [14]; $19.0^{+8.6}_{-6.9}$ [10]; 20.5 [5]; 25.8 [6]; 36.5 [7]; 56.2 [7]; $250 \pm 85$ [9]; $235 \pm 85$ [9]; $478 \pm 175$ [9]; $3.84 \pm 1.25$ [9]
$\Lambda_b \rightarrow p\tau^-\bar{\nu}_\tau$	9.6	4.01 [13]; 6.55 [13]; $312 \pm 105$ [9]; $208 \pm 70$ [9]; $646 \pm 215$ [9]; $1.93 \pm 0.70$ [9]

TABLE VII. Decay widths  $\Lambda_c \rightarrow n\ell^+\nu_\ell$  (in units of  $|V_{cd}|^2 \text{ ps}^{-1}$ ).

Mode	Our result	Theoretical predictions
$\Lambda_c \rightarrow ne^+\nu_e$	0.20	0.26 [12]; 0.20 [13]; 0.27 [13]; $8.21 \pm 2.80$ [9]; $3.82 \pm 1.20$ [9]; $14.40 \pm 5.50$ [9]; $2.51 \pm 0.85$ [9]
$\Lambda_c \rightarrow n\mu^+\nu_\mu$	0.19	0.26 [12]; 0.20 [13]; 0.27 [13]; $8.30 \pm 2.85$ [9]; $3.88 \pm 1.25$ [9]; $14.60 \pm 5.50$ [9]; $2.51 \pm 0.85$ [9]

$\Lambda_c \rightarrow n$  case the effective dipole mass is about 50% higher than the average of the  $D, D^*$  meson masses.

In Tables III and IV we list our form factor results for  $q^2 = 0$  and  $q^2 = q_{\max}^2$  and compare them to the results of the light-front diquark model calculation of [14] and the QCD light-cone sum rules of [10].

It is interesting to explore how the present form factors are related to the corresponding charged or neutral current form factors  $\Lambda_Q \rightarrow \Lambda$ . In the limit of  $SU(3)$  the  $\Lambda_Q \rightarrow \Lambda$  and  $\Lambda_Q \rightarrow N$  ( $N = p, n$ ) form factors are related by  $F(\Lambda_Q \rightarrow \Lambda) = \sqrt{2/3}F(\Lambda_Q \rightarrow N)$ . This can be seen by using the  $\bar{3} \otimes 3 \rightarrow 8$  Clebsch-Gordan (CG) table listed in [33]. Based on the observation that the  $[ud]$  diquark is the ( $Y = 2/3, I = 0$ ) member of the  $\bar{3}$  multiplet, one needs the CG coefficients

$$\begin{aligned} \Lambda_Q \rightarrow \Lambda: & \left\langle \bar{3}, -\frac{2}{3}, 0, 0; 3, \frac{2}{3}, 0, 0 \middle| 8, 0, 0, 0 \right\rangle = \sqrt{2/3}, \\ \Lambda_Q \rightarrow N: & \left\langle \bar{3}, \frac{2}{3}, 0, 0; 3, \frac{1}{3}, \frac{1}{2}, \frac{1}{2} \middle| 8, 1, \frac{1}{2}, \frac{1}{2} \right\rangle = 1. \end{aligned} \quad (24)$$

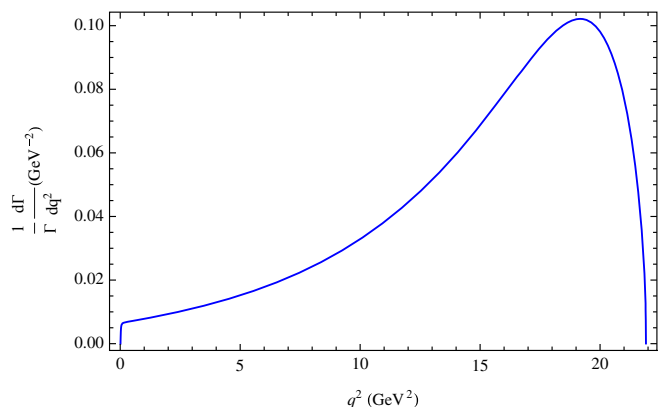
The labeling in (24) proceeds according to the sequence  $\langle \mathbf{R}, Y, I, I_z \rangle$  where  $\mathbf{R}$  denotes the relevant  $SU(3)$  representation. As a check on our calculations we have obtained the

TABLE VIII. Asymmetry parameter  $\alpha_{FB}^\ell$ .

Mode	Our result
$\Lambda_b \rightarrow pe^-\bar{\nu}_e$	-0.388
$\Lambda_b \rightarrow p\mu^-\bar{\nu}_\mu$	-0.388
$\Lambda_b \rightarrow p\tau^-\bar{\nu}_\tau$	-0.434
$\Lambda_c \rightarrow ne^+\nu_e$	0.236
$\Lambda_c \rightarrow n\mu^+\nu_\mu$	0.209

same result analytically in the  $SU(3)$  limit by setting  $\Lambda_{\Lambda_s} = \Lambda_N, M_\Lambda = M_N, m_s = m_u$ .

Our predictions for the branching ratios of the heavy-to-light transitions are listed in Table V. In Tables VI and VII we compare our results for the rates [in units of  $(|V_{qq}|^2 \text{ ps}^{-1})$ ] with the predictions of other theoretical approaches. We use the compilations of results given in Ref. [9]. Most of the approaches give predictions of the same order of magnitude for the decay rates. The only sizable disagreement (up to 2 orders of magnitude) occurs for the full calculations (the first two entries) of Ref. [9] for bottom-to-light baryon transitions. The results of Ref. [9] were obtained in the framework of light-cone QCD sum rules. The last two entries taken from [9] refer to the heavy quark mass limit and show strong deviations from their full results. The results for the lepton-side asymmetry parameters  $\alpha_{FB}^\ell$  are shown in Table VIII.  $q^2$ -distributions for the  $\Lambda_b^0 \rightarrow p\mu^-\bar{\nu}_\mu$  and  $\Lambda_c^+ \rightarrow n\mu^+\nu_\mu$  transition are shown in Figs. 7 and 8.

FIG. 7 (color online).  $q^2$  distribution for the  $\Lambda_b^0 \rightarrow p\mu^-\bar{\nu}_\mu$  transition.

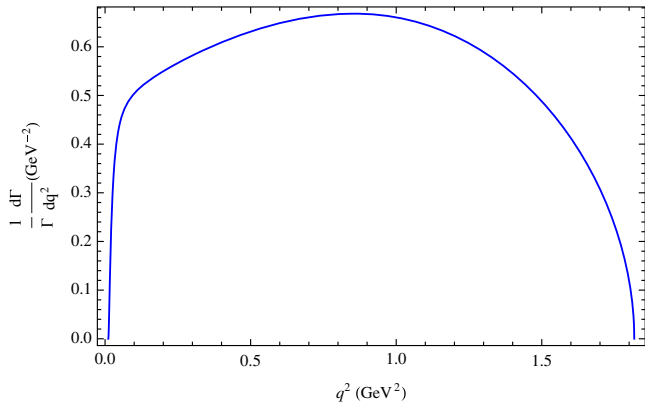


FIG. 8 (color online).  $q^2$  distribution for the  $\Lambda_c^+ \rightarrow n\mu^+\nu_\mu$  transition.

#### IV. SUMMARY

We have used the covariant constituent quark model previously developed by us to calculate semileptonic heavy-to-light transitions of  $\Lambda_b$  and  $\Lambda_c$  baryons. We have

performed a detailed analysis of the invariant and helicity amplitudes, form factors, angular decay distributions, decay widths and asymmetry parameters. Following our previous papers [22,23,26,34] we have used the helicity method in our analysis to provide complete information on the spin structure of the baryons and the off-shell  $W$  boson. We have not provided an analysis of the polarization of the charged lepton which, however, can be obtained in a straightforward manner using the helicity method as described in [26]. Our predictions will be useful for the ongoing experimental study of semileptonic heavy-to-light baryon decays.

#### ACKNOWLEDGMENTS

This work was supported by the DFG under Contract No. LY 114/2-1 and by Tomsk State University Competitiveness Improvement Program. M. A. I. acknowledges the support from Mainz Institute for Theoretical Physics (MITP). M. A. I. and J. G. K. thank the Heisenberg-Landau Grant for support.

- 
- [1] J. Beringer *et al.* (Particle Data Group), *Phys. Rev. D* **86**, 010001 (2012), and 2013 partial update for the 2014 edition.  
[2] K. Abe *et al.* (Belle Collaboration), arXiv:hep-ex/0408145; arXiv:hep-ex/0508018.  
[3] B. Aubert *et al.* (*BABAR* Collaboration), *Phys. Rev. D* **72**, 051102 (2005); arXiv:hep-ex/0506064; arXiv:hep-ex/0507085.  
[4] J. A. Bailey *et al.*, *Phys. Rev. D* **79**, 054507 (2009); E. Gulez, A. Gray, M. Wingate, C. T. H. Davies, G. P. Lepage, and J. Shigemitsu, *Phys. Rev. D* **73**, 074502 (2006); **75**, 119906(E) (2007).  
[5] C.-S. Huang, C.-F. Qiao, and H.-G. Yan, *Phys. Lett. B* **437**, 403 (1998).  
[6] R. S. Marques de Carvalho, F. S. Navarra, M. Nielsen, E. Ferreira, and H. G. Dosch, *Phys. Rev. D* **60**, 034009 (1999).  
[7] M.-Q. Huang and D.-W. Wang, *Phys. Rev. D* **69**, 094003 (2004).  
[8] Y.-M. Wang, Y.-L. Shen, and C.-D. Lu, *Phys. Rev. D* **80**, 074012 (2009).  
[9] K. Azizi, M. Bayar, Y. Sarac, and H. Sundu, *Phys. Rev. D* **80**, 096007 (2009).  
[10] A. Khodjamirian, C. Klein, T. Mannel, and Y. M. Wang, *J. High Energy Phys.* **09** (2011) 106.  
[11] A. Datta, arXiv:hep-ph/9504429.  
[12] M. A. Ivanov, V. E. Lyubovitskij, J. G. Körner, and P. Kroll, *Phys. Rev. D* **56**, 348 (1997).  
[13] M. Pervin, W. Roberts, and S. Capstick, *Phys. Rev. C* **72**, 035201 (2005).  
[14] Z.-T. Wei, H.-W. Ke, and X.-Q. Li, *Phys. Rev. D* **80**, 094016 (2009).  
[15] W. Detmold, C.-J. D. Lin, S. Meinel, and M. Wingate, *Phys. Rev. D* **88**, 014512 (2013).  
[16] T. Branz, A. Faessler, T. Gutsche, M. A. Ivanov, J. G. Körner, and V. E. Lyubovitskij, *Phys. Rev. D* **81**, 034010 (2010).  
[17] S. Dubnicka, A. Z. Dubnickova, M. A. Ivanov, and J. G. Körner, *Phys. Rev. D* **81**, 114007 (2010).  
[18] S. Dubnicka, A. Z. Dubnickova, M. A. Ivanov, J. G. Körner, P. Santorelli, and G. G. Saidullaeva, *Phys. Rev. D* **84**, 014006 (2011).  
[19] M. A. Ivanov, J. G. Körner, S. G. Kovalenko, P. Santorelli, and G. G. Saidullaeva, *Phys. Rev. D* **85**, 034004 (2012).  
[20] T. Gutsche, M. A. Ivanov, J. G. Körner, V. E. Lyubovitskij, and P. Santorelli, *Phys. Rev. D* **86**, 074013 (2012).  
[21] S. Dubnicka, A. Z. Dubnickova, M. A. Ivanov, and A. Liptaj, *Phys. Rev. D* **87**, 074021 (2013).  
[22] T. Gutsche, M. A. Ivanov, J. G. Körner, V. E. Lyubovitskij, and P. Santorelli, *Phys. Rev. D* **87**, 074031 (2013).  
[23] T. Gutsche, M. A. Ivanov, J. G. Körner, V. E. Lyubovitskij, and P. Santorelli, *Phys. Rev. D* **88**, 114018 (2013).  
[24] A. Faessler, T. Gutsche, M. A. Ivanov, J. G. Körner, and V. E. Lyubovitskij, *Phys. Rev. D* **80**, 034025 (2009).  
[25] T. Branz, A. Faessler, T. Gutsche, M. A. Ivanov, J. G. Körner, V. E. Lyubovitskij, and B. Oexl, *Phys. Rev. D* **81**, 114036 (2010).  
[26] A. Kadeer, J. G. Körner, and U. Moosbrugger, *Eur. Phys. J. C* **59**, 27 (2009).  
[27] M. A. Ivanov, M. P. Locher, and V. E. Lyubovitskij, *Few Body Syst.* **21**, 131 (1996); M. A. Ivanov, J. G. Körner, and V. E. Lyubovitskij, *Phys. Lett. B* **448**, 143 (1999);

- M. A. Ivanov, J. G. Körner, V. E. Lyubovitskij, and A. G. Rusetsky, *Phys. Rev. D* **60**, 094002 (1999); M. A. Ivanov, J. G. Körner, V. E. Lyubovitskij, M. A. Pisarev, and A. G. Rusetsky, *Phys. Rev. D* **61**, 114010 (2000); M. A. Ivanov, J. G. Körner, V. E. Lyubovitskij, and A. G. Rusetsky, *Phys. Lett. B* **476**, 58 (2000); A. Faessler, Th. Gutsche, M. A. Ivanov, J. G. Körner, V. E. Lyubovitskij, D. Nicmorus, and K. Pumsa-ard, *Phys. Rev. D* **73**, 094013 (2006); A. Faessler, T. Gutsche, B. R. Holstein, M. A. Ivanov, J. G. Körner, and V. E. Lyubovitskij, *Phys. Rev. D* **78**, 094005 (2008).
- [28] B. L. Ioffe, *Z. Phys. C* **18**, 67 (1983); B. L. Ioffe and A. V. Smilga, *Nucl. Phys.* **B232**, 109 (1984).
- [29] S. Weinberg, *Phys. Rev.* **130**, 776 (1963).
- [30] A. Salam, *Nuovo Cimento* **25**, 224 (1962).
- [31] K. Hayashi, M. Hirayama, T. Muta, N. Seto, and T. Shirafuji, *Fortschr. Phys.* **15**, 625 (1967).
- [32] G. V. Efimov and M. A. Ivanov, *The Quark Confinement Model of Hadrons* (IOP Publishing, Bristol, 1993).
- [33] T. A. Kaeding, [arXiv:nucl-th/9502037](https://arxiv.org/abs/nucl-th/9502037).
- [34] A. Faessler, T. Gutsche, M. A. Ivanov, J. G. Körner, and V. E. Lyubovitskij, *Eur. Phys. J. direct C* **4**, 18 (2002).